Shape coexistence and triaxiality in nuclei near ^{80}Zr

S. J. Zheng,[1,2] F. R. Xu,[1,3,*] S. F. Shen,[4,5,†] H. L. Liu,[1] R. Wyss,[6] and Y. P. Yan[5]

[1]*School of Physics and State Key Laboratory of Nuclear Physics and Technology, Peking University, Beijing 100871, China*
[2]*Key Laboratory of Particle Astrophysics, Institute of High Energy Physics, Chinese Academy of Sciences, Beijing 100049, China*
[3]*Center of Theoretical Nuclear Physics, National Laboratory of Heavy Ion Accelerator of Lanzhou, Lanzhou 730000, China*
[4]*Key Laboratory of Neutronics and Radiation Safety, Institute of Nuclear Energy Safety Technology, Chinese Academy of Sciences, Hefei 230031, Anhui, China*
[5]*School of Physics, Suranaree University of Technology, Nakhon Ratchasima 30000, Thailand*
[6]*AlbaNova University Center, Royal Institute of Technology, S-106 91 Stockholm, Sweden*

(Received 21 August 2014; revised manuscript received 10 November 2014; published 9 December 2014)

Total-Routhian-surface calculations have been performed to investigate the shape evolutions of $A \sim 80$ nuclei: $^{80-84}$Zr, $^{76-80}$Sr, and ^{84,86}Mo. Shape coexistences of spherical, prolate, and oblate deformations have been found in these nuclei. Particularly for the nuclei ^{80}Sr and ^{82}Zr, the energy differences between two shape-coexisting states are less than 220 keV. At high spins, the $g_{9/2}$ shell plays an important role in shape evolutions. It has been found that the alignment of the $g_{9/2}$ quasiparticles drives nuclei to be triaxial.

DOI: 10.1103/PhysRevC.90.064309 PACS number(s): 21.10.−k, 21.60.−n, 27.50.+e

I. INTRODUCTION

The $A \sim 80$ nuclei far from the β-stability line are attracting significant attention because of various shape evolutions and shape coexistences. Moreover, they locate at the key points in the rp (rapid proton capture)-process path, playing an important role in astrophysical nuclear synthesization. According to mean-field models, single-particle level densities in this mass region are noticeably low. There are significant shell gaps at the prolate deformation $\beta_2 \approx 0.4$ with the particle number 38 or 40 and at oblate deformation $\beta_2 \approx -0.3$ with the particle number 34 or 36, which leads to rich shape transitions with changing nucleon numbers. Up to date, the shape coexistence of prolate, oblate, and triaxial deformations has been seen in ^{82}Sr [1]. Superdeformed bands in $^{80-83}$Sr, $^{82-84}$Y, and ^{83,84,86}Zr have been established experimentally (see Ref. [2] and references therein). Some of superdeformed bands in ^{86}Zr [3] and ^{80}Sr [4] are suggested to be triaxial. Theoretical calculations predicted that ^{80}Sr and ^{84}Zr have triaxial deformations [5,6]. Also global calculations with the axial asymmetry shape have been carried out recently for the ground states of the nuclei [7]. The $A \sim 80$ nuclei lie in the region where axial symmetry is broken usually. However, it is not easy experimentally to deduce the information about the triaxial deformation. The wobbling, which has been observed in ^{163,165,167}Lu [8–10], has been considered to be proof of triaxiality. With the advance of experimental techniques, detailed observations in this mass region have become available.

It is predicted that $A \sim 80$ nuclei could contain higher-order geometrical symmetry, such as possible tetrahedral deformation in ground and low-excited states [11]. The exotic deformation correlation comes from the special shell structure [11], giving rich shape information. Though there could be many elements (e.g., pairing correlation) affecting the deformation, the shell structure in the deformed potential governs the shape development of nuclear states. In the present work, we focus on the deformation evolutions and shape coexistences in $A \sim 80$ nuclei.

II. THE MODEL

Total-Routhian-surface (TRS) calculations [12] have been performed. The total Routhian $E^{\omega}(Z,N,\hat{\beta})$ of a nucleus (Z,N) at rotational frequency ω and deformation $\hat{\beta}$ is calculated as follows [12]:

$$E^{\omega}(Z,N,\hat{\beta}) = E^{\omega=0}(Z,N,\hat{\beta}) + [\langle\Psi^{\omega}|\hat{H}^{\omega}|\Psi^{\omega}\rangle - \langle\Psi^{\omega}|\hat{H}^{\omega}|\Psi^{\omega}\rangle_{\omega=0}], \quad (1)$$

where $E^{\omega=0}(Z,N,\hat{\beta})$ is the total energy at zero frequency, consisting of the macroscopic liquid-drop energy [13], the microscopic shell correction [14,15], and the pairing energy [16]. The last two terms in the bracket represent the change in energy due to the rotation. The total Hamiltonian is written as [12]

$$\hat{H}^{\omega} = \sum_{ij}[(\langle i|h_{\rm ws}|j\rangle - \lambda\delta_{ij})a_i^{+}a_j - \omega\langle i|\hat{j}_x|j\rangle a_i^{+}a_j] - G\sum_{i,i'>0} a_i^{+}a_{\bar{i}}^{+}a_{i'}a_{\bar{i}'}. \quad (2)$$

For the single-particle Hamiltonian, $h_{\rm ws}$, a nonaxial deformed Woods-Saxon (WS) potential has been adopted.

The pairing is treated by the Lipkin-Nogami approach [16] in which the particle number is conserved approximately and thus the spurious pairing phase transition encountered in the BCS calculation can be avoided (see Ref. [16] for a detailed description of the cranked Lipkin-Nogami TRS method). Both monopole and quadruple pairings are considered [17] with the monopole pairing strength G determined by the average gap method [18] and quadruple strengths obtained by restoring the Galilean invariance broken by the seniority pairing force [17,19,20]. The TRS calculation is performed in the deformation space $\hat{\beta} = (\beta_2,\gamma,\beta_4)$. Pairing correlations

*frxu@pku.edu.cn
†shuifa.shen@fds.org.cn

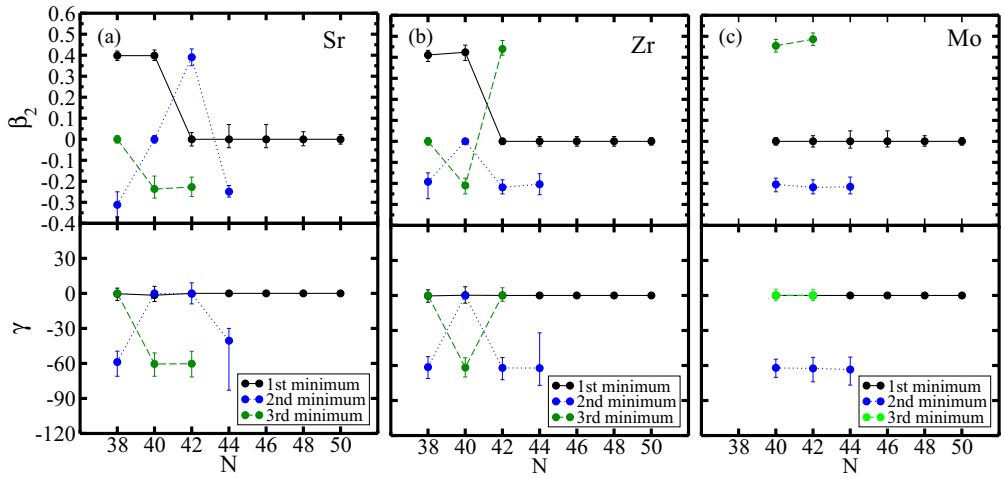

FIG. 1. (Color online) Calculated quadrupole deformations β_2 and γ for even-even Sr, Zr, and Mo isotopes with $38 \leq N \leq 50$. The error bar displays the deformation values within an energy range of less than 100 keV above the minimum, giving an indication of the softness of the nucleus with respect to the corresponding shape parameter. The black dots represent ground-state deformations (first minimum). The blue and green dots represent the coexisting deformations (second and third minimum).

are dependent on the rotational frequency and deformation. To include such dependence in the TRS, we have run the pairing-deformation-frequency self-consistent TRS calculation, i.e., for any given deformation and frequency, pairing is self-consistently treated by the Hartree-Fock-Bogolyubov-like equation [16]. At a given frequency, the deformation of a state is determined by minimizing the calculated TRS.

For $N = Z$ nuclei, the neutron-proton pairing can be remarkable [21,22]. In the present work, however, we are interested in the shape of the nuclei. The pairing correlation should not affect the deformation significantly. The shell correction dominates the shape of a state.

III. CALCULATIONS AND DISCUSSIONS

The TRS calculations for even-even Sr, Zr, and Mo isotopes near $A = 80$ have been performed. Deformations, shape coexistences, and collective rotational properties with increasing rotational frequency are discussed. The kinematic moments of inertia are calculated and compared with existing experimental data.

A. Deformations and shape coexistences in ground and low-lying states

Due to the large shell gaps at prolate, oblate deformations, there is a competition between different deformations. The calculated deformations with (β,γ) of ground states and excited states for even-even Sr, Zr, and Mo isotopes are shown in Fig. 1. Softnesses which indicate the stability of deformations are also calculated and shown. Various shape coexisting states with spherical, prolate, oblate, and triaxial deformations are found in this mass region.

TRS calculations show that the nuclei with $N \leqslant 40$ have well-deformed ($\beta_2 \approx 0.4$) prolate ground states, which is consistent with the experimental data $\epsilon_2 = 0.4$ and $\epsilon_2 = 0.39$ ($\epsilon_2 \approx 0.944\beta_2 - 0.122\beta_2^2 + 0.154\beta_2\beta_4 - 0.199\beta_4^2$) for ^{78}Sr [23] and ^{80}Zr [24], respectively. With the neutron number N approaching the magic number 50, the shapes of the nuclei become spherical. The transitional nuclei between the well-deformed and spherical nuclei are quite soft. Experimentally, γ vibrational bands have been observed for ^{80,82}Sr, ^{82,84}Zr, and ^{86}Mo [25–29], indicating soft deformations. The energy ratios $E(4^+)/E(2^+)$, which indicate the degrees of collectivity, show a similar trend. They decrease steadily from more than 2.80, through 2.5 to 2.3, for $N = 40$, 42, and 44 isotones, respectively, showing the decreasing collectivity.

For strontium isotopes, a shape transition of the ground-state deformations occurs from prolate at $N = 40$ to spherical at $N = 42$. Due to the large shell gaps at prolate, oblate, and spherical shapes, there is a competition between different deformations. Consequently, prolate, oblate and spherical shapes coexist as shown in Fig. 1(a). The nuclei ^{76,78}Sr have well-deformed prolate ground states with $\beta_2 \approx 0.4$. Shallow oblate deformations with $\beta_2 = -0.31$ (^{76}Sr) and $\beta_2 = -0.24$ (^{78}Sr) coexist, which are about 2.04 and 1.53 MeV higher for ^{76}Sr and ^{78}Sr, respectively. The nucleus ^{80}Sr has a spherical ground state. However, it has very low-lying states of prolate ($\beta_2 = 0.39$) and oblate ($\beta_2 = -0.23$) deformations, which are only 70 and 290 keV higher than the ground state. A triaxial shape with $(\beta_2,\gamma) = (0.25, -40^\circ)$ exists in ^{82}Sr, while it is rather soft in the γ direction from -80° to -30°. The γ vibrational band in ^{82}Sr has been observed [26], indicating the soft γ deformation.

A shape transition from prolate to spherical shapes also occurs for the zirconium isotopes as shown in Fig. 1(b). Similar with the strontium isotopes, prolate, oblate, and spherical deformations coexist for the nuclei ^{78,80,82}Zr, while the energy differences between the prolate and oblate deformations vary from 2.02 MeV through 1.28 to -0.112 MeV for ^{78}Zr, ^{80}Zr, and ^{82}Zr, respectively.

For the molybdenum isotopes, spherical shapes become the ground states, while coexistence of prolate or oblate deformation also appears for the nuclei ^{82,84,86}Mo as shown in Fig. 1(c). For the $Z = N$ nucleus ^{84}Mo, little is known

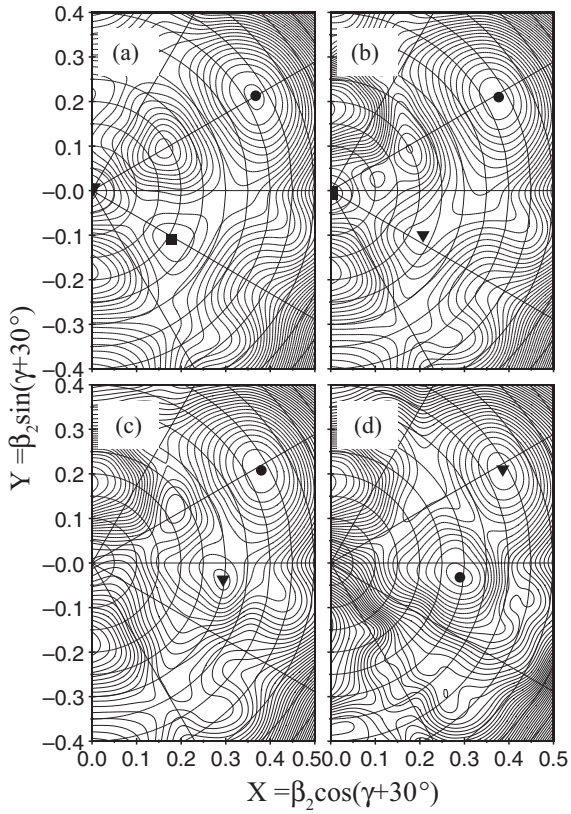

FIG. 2. The total Routhian surfaces for ^{80}Zr at $\hbar\omega = 0.0$ MeV (a), 0.45 MeV (b), 0.55 MeV (c), and 0.7 MeV (d). The solid dots represent the first minima. The solid down-triangles and squares represent the second and third minima, respectively. Contours are at a 200-keV interval.

about the shape information up to date. Several calculations have predicted different shapes. Möller and Nix [30] predicted an oblate deformation with $\varepsilon_2 = -0.18$ ($\varepsilon_2 = 0.95\beta_2$). Nazarewicz *et al.* [5] found it to be soft axially symmetric. A nearly spherical ground state is calculated by Aberg [31]. Petrovici *et al.* [32] predicted it to be prolate with an oblate deformation coexisting above 3 MeV higher. In our calculations, the ground state is spherical and an oblate shape coexists which is only 420 keV higher. Also a highly deformed prolate shape appears with an even higher energy (more than 1.5 MeV).

It should be pointed out here that in many cases the energy differences between coexisting minima are low (less than 1 MeV). In such cases, the interaction between these different shapes is strong and should be taken into account. This is very interesting and will become an important task in the future, but this is a difficult and challenging subject.

B. Triaxial deformations in neutron-deficient Sr, Zr, and Mo isotopes at high spins

Experimental data for ^{80}Zr are very sparse because it is approaching the proton dripline, while its characteristics are crucial and play an important role in the *rp* process. Recently, five cascade transitions have been verified with the ground-state band established up to 10^+ at 3789 keV [33]. Alignment delay has been predicted to appear at higher spins. Neutron-proton pairing interaction may be the cause of the delayed rotational alignment. However, the spin alignment is also sensitively influenced by other factors such as deformation [34]. Thus the shape transitions are discussed in detail for the nuclei of this region.

TRS diagrams for ^{80}Zr are shown in Fig. 2 at specific rotational frequencies, $\hbar\omega = 0.0$, 0.45, 0.55, and 0.70 MeV respectively. At $\hbar\omega = 0$ MeV, that is, for the ground state of the nucleus, a well-deformed prolate shape with $\beta_2 = 0.42$ coexists with an oblate shape as discussed above. As rotational frequency increases, the oblate deformation minimum becomes shallower and it disappears at $\hbar\omega = 0.45$ MeV. Then a stable triaxial shape develops at $\hbar\omega = 0.55$ MeV and its total Routhian energy is lower at higher rotational frequency. At $\hbar\omega \approx 0.7$ MeV it becomes yrast with $I \sim 19\hbar$. Subsequently, the nucleus shows much more stable triaxiality up to $38\hbar$. In the work of Yamagami *et al.* [35], by performing fully three-dimensional (3D) symmetry-unrestricted Skyrme-Hartree-Fock-Bogoliubov calculations, they point out that a low-lying spherical minimum coexisting with the prolate ground state in ^{80}Zr is extremely soft against the Y_{32} tetrahedral deformation, but in our Woods-Saxon (WS) potential, axially symmetric octupole (Y_{30}) and nonaxial octupole (Y_{31}, Y_{32}, Y_{33}) deformation parameters are not included.

Subsequently, the single-quasiparticle Routhians are calculated and shown in Fig. 3 for the prolate and triaxial deformations. For the $N = Z$ nucleus ^{80}Zr, the neutrons and

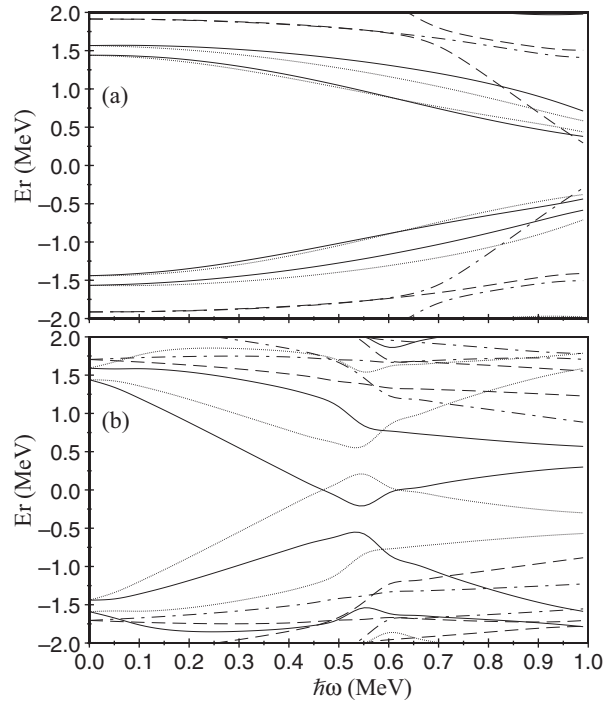

FIG. 3. Quasineutron Routhians of ^{80}Zr for prolate (a) and triaxial (b) deformations with $(\beta_2, \gamma) = (0.424, 0.2^\circ)$ and $(0.297, -37.9^\circ)$, respectively. (π, α): Solid lines represent $(+, +1/2)$, dotted lines represent $(+, -1/2)$, dot-dash lines represent $(-, +1/2)$, and dashed lines represent $(-, -1/2)$

protons occupy the same single-particle orbitals and they have nearly the same Routhians; therefore only quasineutron Routhians are shown. For the prolate deformation, there are no alignments shown. For the triaxial deformation, neutron alignments are predicted to emerge at a rotational frequency of about 0.55 MeV and proton alignments emerge simultaneously. It is considered to be alignments of $g_{9/2}$ quasiprotons and quasineutrons as its neighboring nuclei ^{81}Sr and ^{84}Zr [6,36]. Note that triaxial deformation develops after the alignments as shown in Fig. 2. That is to say, the alignments of four $g_{9/2}$ quasiparticles drive the nucleus to be triaxial. This is consistent with the prediction [37] that the alignment of $g_{9/2}$ proton orbits tends to be a positive γ drive when $Z = 40$. Experimentally, it has been found that the $g_{9/2}$ neutron polarizes the soft core of the nuclei ^{55,57,59}Cr [38] and ^{59}Fe [39]. For the nuclei in the $A = 80$ region, particularly for the nucleus ^{80}Zr, both $g_{9/2}$ proton and neutron orbits are occupied; thus the shape driving effects are strengthened.

Calculations for the neighboring nuclei $^{76-80}$Sr, ^{82,84}Zr, and ^{84,86}Mo are also carried out with the cranking TRS model, showing a similar trend. The triaxially deformed shape develops after the alignments of $g_{9/2}$ quasiprotons and quasineutrons.

The moments of inertia are very sensitive to the nuclear shape. Thus the kinematic moments of inertia are calculated and compared with experimental results as shown in Figs. 4–6, for $^{80-84}$Zr, $^{76-80}$Sr, and ^{84,86}Mo, respectively. The method of converting the sequence of γ rays into moments of inertia is detailed in Ref. [40].

For the nucleus ^{84}Zr, triaxial and prolate (prolate-1 and prolate-2) deformations coexist in our calculations. As can be seen from Fig. 4, the kinematic moments of inertia of the triaxial rotational band agree rather well with the experimental results. They show a steep upbending at the rotational frequency around 0.5 MeV/$\hbar$ due to the alignments of a pair of quasiprotons and quasineutrons. After the alignments, a down slope appears indicating the decreasing deformation which is also in accordance with the triaxial deformation evolving. There are some discrepancies between the experimental results and our calculations at low spins for the nucleus ^{82}Zr because the deformation is considerably soft as discussed above. At higher spins after the band crossing, a stable triaxial deformation appears and the resulting kinematic moments of inertia of triaxiality agree well with the experiment. Experimental data for ^{80}Zr are limited and it is impossible to show any trend at high rotational frequency. However, the observed upbending behavior agrees well with the calculated prolate band with frequency energy lower than 0.6 MeV. A triaxially deformed band is predicted, which also exhibits a downbending behavior and becomes yrast at higher rotational frequency.

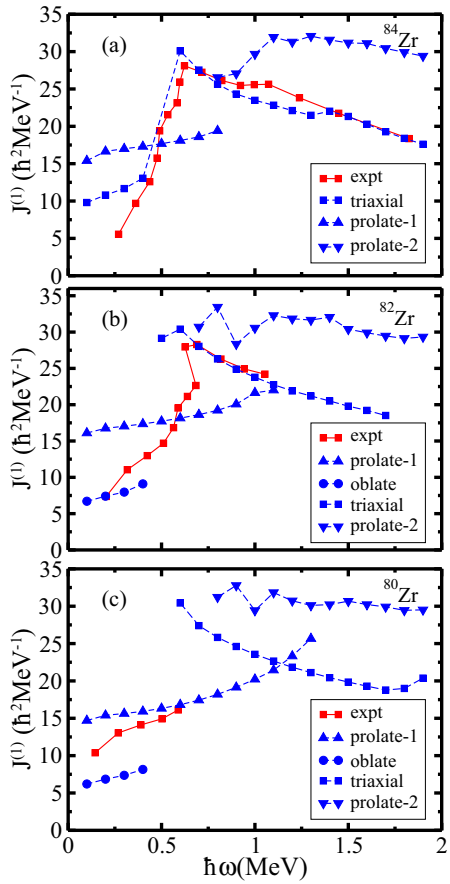

FIG. 4. (Color online) Kinematic moments of inertia for ^{84}Zr, ^{82}Zr, and ^{80}Zr as functions of the rotational frequency.

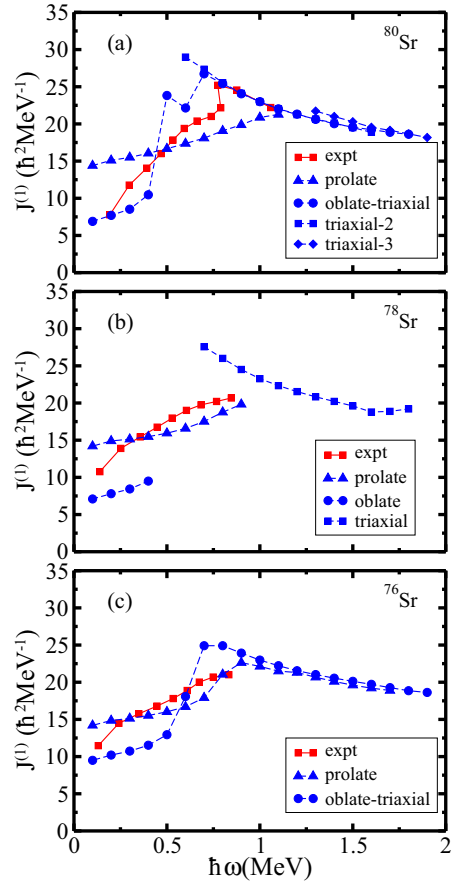

FIG. 5. (Color online) Kinematic moments of inertia for ^{80}Sr, ^{78}Sr, and ^{76}Sr as functions of the rotational frequency.

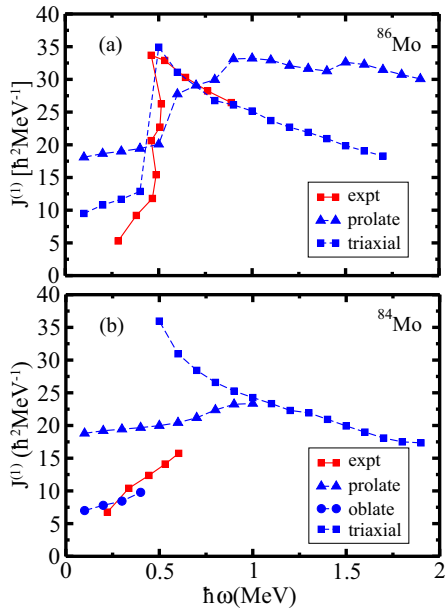

FIG. 6. (Color online) Kinematic moments of inertia for ^{84}Mo and ^{86}Mo as functions of the rotational frequency.

Plots of the kinematic moments of inertia versus rotational frequency for strontium and molybdenum isotopes shown in Figs. 5 and 6 also show good consistence between the experimental results and calculations. At high spins, the triaxially deformed shapes appear and become stable after the alignments. For the nucleus ^{80}Sr, it is even complicated at high spins. Varieties of shapes such as prolate, oblate-triaxial, triaxial-2, and triaxial-3 (shown in Fig. 5) coexist. They have the nearly same moments of inertia and also similar total Routhians, indicating that several different configurations are available at high spins. For the nucleus ^{84}Mo, only a few experimental data are available, while it behaves like an oblate band at low spins. At the rotational frequency of $\hbar\omega \approx 0.5$ MeV, a shape transition from oblate to triaxial deformation is predicted and it will keep stable up to $24\hbar$.

IV. SUMMARY

In conclusion, the nuclei with mass number around 80, i.e., $^{76-80}$Sr, $^{80-84}$Zr, and ^{84,86}Mo, have been calculated by the TRS model. Due to the large gaps at the prolate deformation $\beta_2 \approx 0.4$ with the particle number 38 or 40 and gaps at oblate deformation $\beta_2 \approx -0.3$ with the particle number 34 or 36, shape coexistences are prominent in this region. Spherical, prolate, oblate, and triaxial deformations coexist. Mostly, prolate and oblate deformations coexist at low spins while the energy difference between the two shapes deviates largely. For the nuclei ^{76,78}Sr and ^{78,80}Zr, the Routhians of the prolate deformations are lower than the oblate ones by more than 1 MeV, while for the nuclei ^{80}Sr and ^{82}Zr, the energy differences between the two deformations are less than 220 keV.

At high spins, due to the alignments of a pair of $g_{9/2}$ protons and a pair of $g_{9/2}$ neutrons, triaxial deformations develop. Both ^{82}Zr and ^{84}Zr show stable triaxial deformations after the alignments. The triaxially deformed shape for ^{80}Zr is predicated to develop at high spins. The neighboring nuclei $^{76-80}$Sr and ^{84,86}Mo also show triaxiality at high spins. Thus the $g_{9/2}$ orbits play a particular role in the shape transitions of nuclei in this region.

ACKNOWLEDGMENTS

This work is supported by the Major State Basic Research Development Program in China under Contract No. G2000077400, the National Natural Science Foundation of China under Grants No. 10175002, No. 11065001, and No. 10475002, the Doctoral Foundation of Chinese Ministry of Education under Grant No. 20030001088, the Foundation of the Education Department of Jiangxi Province under Grant No. GJJ12372, and Suranaree University of Technology under Contract No. 15/2553.

[1] C. Baktash *et al.*, Phys. Lett. B **255**, 174 (1991).
[2] F. Lerma *et al.*, Phys. Rev. C **67**, 044310 (2003).
[3] D. G. Sarantites *et al.*, Phys. Rev. C **57**, R1 (1998).
[4] M. Devlin *et al.*, Phys. Lett. B **415**, 328 (1997).
[5] W. Nazarewicz, J. Dudek, R. Bengtsson, T. Bengtsson, and I. Ragnarsson, Nucl. Phys. A **435**, 397 (1985).
[6] J. Dudek, W. Nazarewicz, and N. Rowley, Phys. Rev. C **35**, 1489 (1987).
[7] P. Möller, R. Bengtsson, B. G. Carlsson, P. Olivius, and T. Ichikawa, Phys. Rev. Lett. **97**, 162502 (2006).
[8] D. R. Jensen *et al.*, Phys. Rev. Lett. **89**, 142503 (2002).
[9] G. Schönwaßer *et al.*, Phys. Lett. B **552**, 9 (2003).
[10] H. Amro *et al.*, Phys. Lett. B **553**, 197 (2003).
[11] J. Dudek, A. Goźdź, N. Schunck, and M. Miśkiewicz, Phys. Rev. Lett. **88**, 252502 (2002).
[12] W. Nazarewicz, R. Wyss, and A. Johnson, Nucl. Phys. A **503**, 285 (1989).
[13] W. D. Myers and W. J. Swiatecki, Nucl. Phys. **81**, 1 (1966).
[14] W. Nazarewicz, M. A. Riley, and J. D. Garrett, Nucl. Phys. A **512**, 61 (1990).
[15] V. M. Strutinsky, Yad. Fiz. **3**, 614 (1966); Nucl. Phys. A **95**, 420 (1967).
[16] W. Satuła, R. Wyss, and P. Magierski, Nucl. Phys. A **578**, 45 (1994).
[17] W. Satuła and R. Wyss, Phys. Rev. C **50**, 2888 (1994).
[18] P. Möller and J. R. Nix, Nucl. Phys. A **536**, 20 (1992).
[19] H. Sakamoto and T. Kishimoto, Phys. Lett. B **245**, 321 (1990).
[20] F. R. Xu, W. Satuła, and R. Wyss, Nucl. Phys. A **669**, 119 (2000).
[21] R. A. Wyss and W. Satuła, Acta Phys. Pol. B **32**, 2457 (2001).
[22] W. Satuła and R. Wyss, Phys. Lett. B **393**, 1 (1997).
[23] C. J. Lister, B. J. Varley, H. G. Price, and J. W. Olness, Phys. Rev. Lett. **49**, 308 (1982).
[24] C. J. Lister *et al.*, Phys. Rev. Lett. **59**, 1270 (1987).
[25] T. A. Sienko, C. J. Lister, and R. A. Kaye, Phys. Rev. C **67**, 064311 (2003).
[26] S. L. Tabor, J. Döring, J. W. Holcomb, G. D. Johns, T. D. Johnson, T. J. Petters, M. A. Riley, and P. C. Womble, Phys. Rev. C **49**, 730 (1994).
[27] D. Rudolph *et al.*, Phys. Rev. C **56**, 98 (1997).
[28] J. Döring *et al.*, Phys. Rev. C **67**, 014315 (2003).

[29] K. Andgren *et al.*, Phys. Rev. C **76**, 014307 (2007).
[30] P. Möller and J. R. Nix, Nucl. Phys. A **361**, 117 (1981).
[31] S. Aberg, Phys. Scr. **25**, 23 (1982).
[32] A. Petrovici, K. W. Schmid, and Amand Faessler, Nucl. Phys. A **605**, 290 (1996).
[33] S. M. Fischer *et al.*, Phys. Rev. Lett. **87**, 132501 (2001).
[34] N. Mărginean *et al.*, Phys. Rev. C **65**, 051303 (2002).
[35] M. Yamagami, K. Matsuyanagi, and M. Matsuo, Nucl. Phys. A **693**, 579 (2001).
[36] E. F. Moore, P. D. Cottle, C. J. Gross, D. M. Headly, U. J. Hüttmeier, S. L. Tabor, and W. Nazarewicz, Phys. Rev. C **38**, 696 (1988).
[37] W. D. Luo and Y. S. Chen, Nucl. Phys. A **564**, 413 (1993).
[38] A. N. Deacon *et al.*, Phys. Lett. B **622**, 151 (2005).
[39] A. N. Deacon *et al.*, Phys. Rev. C **76**, 054303 (2007).
[40] R. Bengtsson and S. Frauendorf, Nucl. Phys. A **327**, 139 (1979).